Lawrence Berkeley National Laboratory
Recent Work

Title
PHOTOCHEMISTRY OF NOx AND HNOx COMPOUNDS

Permalink
https://escholarship.org/uc/item/02r5p6kg

Authors
Johnston, Harold S.
Graham, Richard.

Publication Date
1973-10-01

PHOTOCHEMISTRY OF NO_x AND HNO_x COMPOUNDS

Harold S. Johnston and Richard Graham

October 1973

DISCLAIMER

Photochemistry of NO_x and HNO_x Compounds

Harold S. Johnston and Richard Graham

Department of Chemistry
University of California
and
Inorganic Materials Research Division
Lawrence Berkeley Laboratory
Berkeley, California

Abstract

Cross sections for absorption of radiation between 190 and 700 nm are given for N_2O, NO_2, NO_3, N_2O_4, N_2O_5, HNO_2, and HNO_3. The quantum yields and the primary products of photolysis of each of these substances are discussed. This article includes spectral data obtained in this laboratory for NO_2, NO_3, N_2O_5, HNO_2, and HNO_3 and it includes spectral data from the literature for N_2O and N_2O_4. The quantum yields are based both on results from this laboratory and from the literature.

Introduction

The photolysis of the oxides of nitrogen and of the oxyacids of nitrogen involves the absorption cross section σ and the primary quantum yield ϕ, each a function of wave length. The cross section σ is defined at the average wave length λ by

$$\ln I_o(\lambda)/I(\lambda) = \sigma(\lambda)[A]L$$

where [A] is the concentration of substance A in molecules cm^{-3}, L is the optical path length in cm, I_o is the incident beam over the narrow wavelength band in units of photons $cm^{-2} \ sec^{-1}$, and I is the transmitted intensity. The cross section σ is in units of cm^2, depends on wavelength λ, and for broadbands of radiation depends on the band width of radiation $\Delta\lambda$. The quantum yield for photolysis of A is the ratio of molecules of A destroyed per photon of radiation absorbed

$$\phi = \frac{\text{molecules of A destroyed}}{\text{photons of radiation absorbed}}$$

The quantum yield for forming a given product P is the ratio of the number of molecules of P formed per photon of radiation absorbed by A.

This article briefly reviews the literature for absorption cross sections of N_2O (190-315 nm), HNO_3 (190-325 nm), N_2O_4 (240-390 nm), N_2O_5 (285-380 nm); and it presents data from this laboratory for NO_2 (190-420 nm), N_2O_5 (205-285 nm), HNO_2 (300-397 nm), and NO_3 (450-680 nm). This article briefly reviews

the literature for the quantum yields for photolysis of N_2O, NO_2, N_2O_4, and N_2O_5; and it presents data from this laboratory for the quantum yields of HNO_3 and HNO_2. The possible photolysis products of NO_3 are discussed. This article does not discuss nitric oxide (NO), which is a separate, full-sized research problem all in itself and which is being analyzed by others.

The purpose of this article is to collect in one place the values of cross section σ and quantum yield ϕ. The cross sections are given in Tables 1 to 3 and in Figures 1 to 5. The quantum yields are indicated on some of the figures and are discussed separately for each case.

Experimental

The apparatus has been described previously (1). It consists of a silica cell 15 cm in diameter and 2 meters long. It is equipped with nickel-coated stainless-steel end caps and with three mirrors to give multiple pass operation (White cell). Spectra were taken with optical paths between 8.6 and 34 meters. Deuterium arc sources were used for radiation between 190 and 420 nm, and tungsten filament sources were used above 420 nm. Wave lengths were calibrated from a low-pressure mercury arc. A McPherson one-third meter vacuum spectrometer was used.

Materials.--Oxygen was purified by passing through a column containing pellets of 5% palladium on alumina at 350°C, through a silica tube with copper turnings at 600°C, and then through columns of ascarite and phosphoric anhydride (P_2O_5). Ozone was prepared by electric discharge through purified oxygen; it was collected on silica gel at Dry Ice temperature and degassed at higher temperatures either into a helium carrier or into a vacuum. Nitric oxide was purified by the method of Dinerman and Ewing (2). Nitrogen dioxide was purified as previously described (1). Dinitrogen pentoxide was prepared from nitrogen dioxide and ozone by the reaction

$$2NO_2 + O_3 \rightarrow N_2O_5 + O_2$$
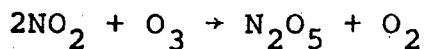
The NO_3 radical was prepared in a low, steady state concentration by mixing N_2O_5 with an excess of ozone; in this system ozone undergoes a slow, catalytic decomposition. Nitrous acid vapor was prepared at a low equilibrium concentration in a system with excess NO, small amounts of H_2O, and very small amounts of NO_2

$$NO + NO_2 + H_2O = 2HNO_2$$
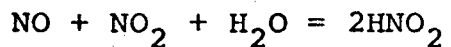
Discussion of Each Substance

Nitrous oxide.--The absorption cross sections for N_2O were read from a graph by Bates and Hayes (3). These cross sections are entered in Table 1 and on Figures 1 and 2. The photolysis of nitrous oxide can give the following products as a function of wavelength

(a) $N_2O + h\nu \rightarrow N_2 (X\ ^1\Sigma) + O(^1D)$ $\lambda < 337$ nm

(b) $\rightarrow N_2 (X\ ^1\Sigma) + O(^1S)$ $\lambda < 210$ nm

(c) $\rightarrow NO (X\ ^2\Pi) + N(^4S)$ $\lambda < 250$ nm

Preston and Barr (4) state that the primary quantum yield for photolysis of nitrous oxide is 1.00 at all wavelengths below 337 nm, and the process forming atomic nitrogen (c) is 0.01 or less.

Nitrogen dioxide.--The photochemistry of NO_2 has been thoroughly reviewed by Hampson and Garvin (5). Here we present our data for the NO_2 spectrum and a summary of Hampson and Garvin's conclusions about quantum yields. The absorption spectrum of NO_2 with 8.6 meter optical path, 1.3 nm resolution (full width at half maximum), averaged over one nm, with $(1\ to\ 10) \times 10^{14}$ molecules cm^{-3}, and at 294°K is given by Figure 2, and values at each 5 nm between 190 and 420 nm are listed in Table 1. The concentration of N_2O_4 is less than 10^{10} molecules cm^{-3} for the points taken below 250 nm, and the contribution of N_2O_4 to the spectrum of NO_2 should be immeasurably small.

Hampson and Garvin (5) concluded that under atmospheric conditions, the primary quantum yield for

(d) $NO_2 + h\nu \rightarrow NO (X\ ^2\Pi) + O(^3P)$
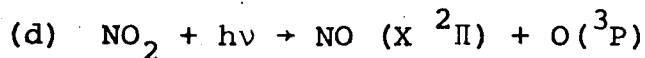
is unity from 398 to 244 nm, and the primary quantum yield for

(e) $NO_2 + h\nu \rightarrow NO (X\ ^2\Pi) + O(^1D)$
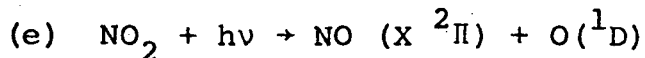
is unity from 244 to 190 nm. There is some temperature and

pressure dependent structure to the quantum yield above 398 nm.
At 298°K, above 398 nm, Hampson and Garvin recommend as primary
quantum yield for formation of $O(^3P)$ the following values:
400, 0.70; 405, 0.29; 410, 0.12; 415, 0.05; 420, 0.02; 425, 0.01;
435, 0.002; 440, 0.001; above 440, zero. Although the threshold
to form $O(^1D)$ is 244 nm, the detailed pattern of quantum yield
as a function of wavelength has not been reported.

Dinitrogen tetroxide.--The absorption spectrum of N_2O_4
was read from a graph by Hall and Blacet (6), and it is entered
in Table 1 from 240 to 390 nm. Although 240 nm is the lowest
wavelength given by Hall and Blacet, there is evidence that
N_2O_4 has a strong absorption below 240 nm.

The photolysis of N_2O_4 can proceed by at least two paths

(f) $N_2O_4 + h\nu \rightarrow NO_2 + NO_2$

(g) $N_2O_4 + h\nu \rightarrow N_2O_3 + O \rightarrow NO + NO_2 + O$
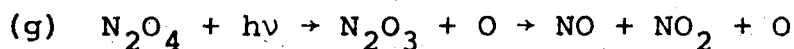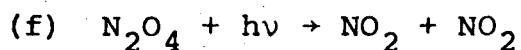
Since NO_2 is in rapid equilibrium with N_2O_4, process (f) would
be rapidly reversible, and would give an apparent quantum yield
of zero. Reaction (g) would be rapidly followed by
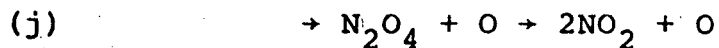
(h) $NO_2 + O \rightarrow NO + O_2$
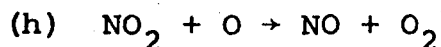
to give a quantum yield of two for formation of nitric oxide.
Holmes and Daniels (7) found the overall quantum yield of NO
was 0.4±0.1 at 265 nm and 0.2±0.1 at 280 nm. Presumably both
processes (f) and (g) occur, and the resulting quantum yield
is an average between zero for one process and two for the other.

Dinitrogen pentoxide.--Dinitrogen pentoxide was prepared
from nitrogen dioxide and ozone. Pure nitrogen pentoxide can
be frozen out of a system containing excess ozone and sublimed
from the white crystals formed. Pure nitrogen pentoxide undergoes
a fairly rapid thermal decomposition (Daniels and Johnston) (8)
to give O_2 and NO_2, which overlaps the N_2O_5 spectrum. The NO_2
bands can be suppressed by excess ozone, but then the N_2O_5
spectrum has the O_3 and the NO_3 spectra superimposed. Starting
with an excess of O_3, we carried out repeated scans of the
spectrum from 200 to 400 nm. The ozone is catalytically decomposed
by the N_2O_5 (Schumacher and Sprenger) (9). For a brief period
O_3 is essentially all gone and little or no NO_2 has appeared.
This spectrum of N_2O_5 is almost free of interference from NO_2
and O_3, and the small amount present can be corrected for, in
terms of the known spectra.

However, a more serious problem was the reaction of N_2O_5
with the walls of the silica vessel to produce some nitric acid.
The amount of nitric acid present was deduced as follows: Excess
ozone was added to a known initial concentration of NO_2 in the
long-path cell. Repeated spectra were taken as the ozone
disappeared, and the repeated spectra continued to be taken as
the N_2O_5 decomposed to NO_2 and O_2. The final concentration
of NO_2 was obtained by extrapolation of the first-order decay
of N_2O_5. The difference between initial NO_2 and final NO_2
was ascribed to nitric acid, HNO_3, whose spectrum is known.
Thus the observed optical density was corrected for small amounts
of O_3 or NO_2 and for relatively large amounts of HNO_3.

The absorption spectrum of 4.1×10^{14} molecules cm^{-3} of N_2O_5, between 205 and 285 nm, 8.6 meter optical path, 1.3 nm resolution, and 295°K, is listed in Table 1 and plotted on Figure 3. In this figure, the effect of 5.5×10^{14} molecules cm^{-3} of HNO_3 has been subtracted. Jones and Wulf (10) have reported N_2O_5 cross sections by means of photographic spectroscopy between 285 and 380 nm. At 285 nm Jones and Wulf obtained a cross section of 5.1×10^{-20} cm^2, and we obtained 4.5×10^{-20} cm^2. The data of Jones and Wulf are included in Table 1 and Figure 3, and they are in satisfactory agreement with our data. The uncertainty in our N_2O_5 spectrum, largely based on the uncertainty in correcting for HNO_3, is estimated to be ±20%.

Studies of the photochemistry of N_2O_5 are greatly complicated by branching paths and by possible secondary chemical reactions. In pure N_2O_5 (almost unobtainable because of the thermal decomposition of N_2O_5 to NO_2) the reasonable primary processes are

(i) $N_2O_5 + h\nu \rightarrow NO_2 + NO_3$

(j) $\rightarrow N_2O_4 + O \rightarrow 2NO_2 + O$

Reaction (j) could be followed by either

(k) $N_2O_5 + O \rightarrow 2NO_3$

(ℓ) $N_2O_5 + O \rightarrow 2NO_2 + O_2$
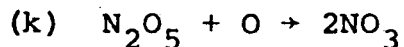
Reaction (i) is reversed by

(m) $NO_2 + NO_3 \xrightarrow{M} N_2O_5$
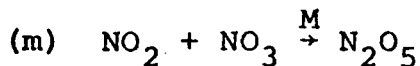
As NO_2 accumulates it may react with the oxygen atom

(h) $NO_2 + O \quad NO + O_2$
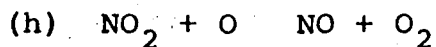
N_2O_5 rapidly reacts with nitric oxide by way of

(o) $N_2O_5 \overset{M}{\rightarrow} NO_2 + NO_3$

(p) $NO + NO_3 \rightarrow 2NO_2$
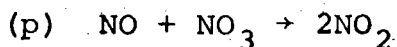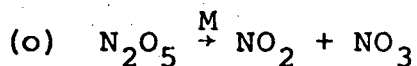
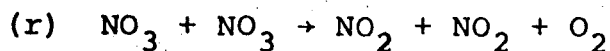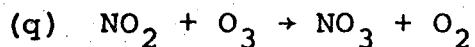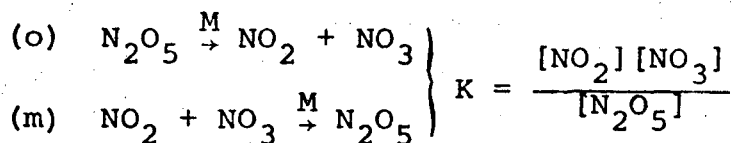The net quantum yield of destruction of N_2O_5 varies with mechanism; _im_, zero; _jkmm_, zero; _jℓ_, 2; _jhop_, 2. Holmes and Daniels (7) observed a quantum yield for loss of N_2O_5 at 280 nm in the absence of NO_2 of about 0.6. Murphy (11), as reported by Hampson (12), found inert-gas dependent quantum yields between 0.3 and 0.6 at 280 nm. Although these low, pressure-dependent quantum yields may be interpreted in terms of long-lived photo-excited N_2O_5, it is also possible (and, we think, more probable) that it is a matter of complex secondary thermal reactions such as (k) through (p).

The primary processes in the photolysis of N_2O_5 are not understood at this time, nor are the secondary reactions of oxygen atoms with N_2O_5 well understood.

The radical NO_3.--The NO_3 radical was prepared in steady state relationship to N_2O_5 and excess O_3. The chemistry of NO_3 is this system has been reviewed in a text book (13). There are four elementary chemical reactions

(o) $N_2O_5 \overset{M}{\rightarrow} NO_2 + NO_3$ ⎞
                           ⎬ $K = \dfrac{[NO_2][NO_3]}{[N_2O_5]}$

(m) $NO_2 + NO_3 \overset{M}{\rightarrow} N_2O_5$ ⎠

(q) $NO_2 + O_3 \rightarrow NO_3 + O_2$

(r) $NO_3 + NO_3 \rightarrow NO_2 + NO_2 + O_2$

The steady-state concentration of NO_3 is

$$[NO_3] = (Kq/2r)^{1/3}[O_3]^{1/3}[N_2O_5]^{1/3}$$

At 300°K, the equilibrium constant K is 1.2×10^{11} molecules cm^{-3}, and the ratio $q/2r$ is 1.7. Thus in units of molecules cm^{-3}, the concentration of NO_3 is

$$[NO_3] = \{1.9 \times 10^{11}[O_3][N_2O_5]\}^{1/3}$$

The absorption spectrum for NO_3 in the visible region (450 to 680 nm) was obtained in a flow system at one atmosphere total pressure. The input gases were nitrogen containing 0.1% NO_2 (and a small amount of NO, which was separately measured and accounted for) and nitrogen plus ozone, as degassed from silica gel. Ozone was present in excess, so that NO and NO_2 were converted to N_2O_5. The amount of residual ozone was determined by its absorption spectrum, corrected for overlapping N_2O_5. For the spectrum presented in Table 2 and in Figure 4, the cell concentrations at 22°C were: O_3, 5.2×10^{16}; N_2O_5, 7.2×10^{14}; NO_3, 1.6×10^{14} molecules cm^{-3}. The NO_3 spectrum has been corrected for the absorption of visible light by ozone.

The absorption spectrum of NO_3 as presented in Table 2 and Figure 4 is estimated to be uncertain by ±50%. This large uncertainty arises from the rate constants q and r entering the expression for the steady-state concentration of NO_3 and in a 15% loss of N_2O_5 that reacted with water in the flowing gases to form nitric acid.

Schott and Davidson (14) measured the absorption coefficient at 652 nm of NO_3 at high temperatures in a shock-tube experiment. They extrapolated their results to 300°K to obtain 8.4×10^{-19} cm^2 as the cross section at 652 nm. We find 2.1×10^{-19} at this wavelength.

To photolyze NO_3 to nitrogen dioxide and a ground state oxygen atom

$$NO_3 + h\nu \rightarrow NO_2 + O(^3P)$$
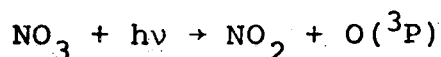
requires a wave length of 578 nm or shorter, and the peaks of maximum absorption lie at longer wave lengths. The radical NO_3 has only slightly less energy (about 5 or 6 kcal $mole^{-1}$) than ground state O_2 and NO. The absorption spectrum in Figure 4 has enough energy to proceed as

$$NO_3 + h\nu \rightarrow NO + O_2 \; (^1\Sigma)$$
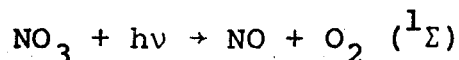
although the state of the products has not been identified. By a molecular modulation technique, we found (work still in progress) that above 600 nm NO_3 dissociates to form NO; and we were unable to detect any fluorescence, which would indicate a low quantum yield. Ramsey (15) found the high resolution spectrum of NO_3 to show predissociation $\underset{\wedge}{\text{at all wavelengths.}}$ Thus above 578 nm, NO_3 is photodissociated to NO and to some form of O_2, probably (but not necessarily) with a large quantum yield; but below 578 nm it is not known whether the products are NO_2 + O or NO + O_2.

Nitrous acid.--HNO_2 was prepared from mixtures of NO, NO_2, H_2O, and He. The concentration of HNO_2 present was calculated from thermochemical data (16) for the equilibrium
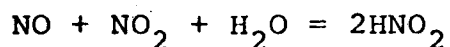
$$NO + NO_2 + H_2O = 2HNO_2$$

$$K = [HNO_2]^2/[NO][NO_2][H_2O]$$

The reactant gases NO and NO_2 were measured from their pressure in small glass pipets, and they were added to the large (46 liter) cell. Helium saturated with water vapor was added. There was a large excess of NO. The actual residual concentration of NO_2 was measured in terms of its known spectrum above 400 nm. The spectrum of N_2O_3 between 300 and 400 nm was obtained in separate experiments, and it was subtracted from the observed total spectrum. Thus the observed relatively weak spectrum of HNO_2 was corrected for the spectrum of NO_2 and the intense continuous spectrum of N_2O_3.

The absorption spectrum of HNO_2 is presented in Table 3 and Figure 5. It was obtained with the following conditions: NO, 2.6×10^{18} molecules cm^{-3}; NO_2, 3.0×10^{15} molecules cm^{-3}; N_2O_3, 8.0×10^{12} molecules cm^{-3}; H_2O, 8.9×10^{15} molecules cm^{-3}; HNO_2 (calc), 6.1×10^{15} molecules cm^{-3}; 294°K; 8.6 meter optical path; 1.3 nm resolution. In other experiments several aliquots of He and H_2O were added to a similar mixture of gases. Beer's law was obeyed over the experimental range of HNO_2, (2 to 8)$\times 10^{15}$ molecules cm^{-3}. The position of the peaks in the spectrum agreed within 0.1 nm of those of King and Moule (17) whose high resolution study of

the HNO_2 spectrum revealed no additional structure. The values of the cross sections in Table 3 and Figure 5 are regarded as uncertain by ±20%, on the basis of uncertainties in the corrections for N_2O_3.

A study of the quantum yield and primary photolysis products of nitrous acid is underway in this laboratory. Preliminary results are given here. Since HNO_2 is unstable in the gas phase, it is necessary to have excess of NO, H_2O, and NO_2 present in the system, with attendant small concentrations of N_2O_4 and N_2O_3 also present. The substances NO_2, N_2O_3, and N_2O_4 all absorb radiation in the same region as HNO_2. Thus it is desirable to minimize NO_2 as much as possible.

The possible primary products of HNO_2 photolysis include

(s) $HNO_2 + h\nu \rightarrow HO + NO$

(t) $\rightarrow H + NO_2$

(u) $\rightarrow HNO + O$
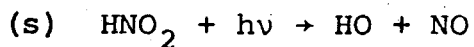
The third alternative would lead to nitrous oxide

$2HNO \rightarrow H_2O + N_2O$
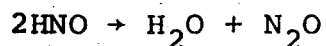
The second alternative would probably be followed by $H + NO_2 \rightarrow HO + NO$, and thus be indistinguishable from the first. The reaction of HO with NO to reform nitrous acid is rapid

$HO + NO \overset{M}{\rightarrow} HNO_2$
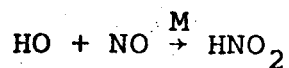
so that no net change would be observed in a static system.

By addition of excess carbon monoxide to the system, the presence of hydroxyl radicals can be identified

$$HO + CO \rightarrow CO_2 + H$$
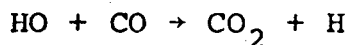
A few experiments have been carried out in which HNO_2 has been photolyzed at 355 nm, and the products have been analyzed by a high resolution mass spectrometer, which could differentiate between N_2O and CO_2. In the absence of added CO, no N_2O was observed. One run was made with the following composition: CO, 8.8×10^{18}; He, 1.0×10^{19}; NO, 4.4×10^{17}; H_2O, 4.4×10^{17}; NO_2, 3.2×10^{16}; and HNO_2, 7.0×10^{16} molecules cm^{-2}. Photolysis was carried out in a quartz cell 3.5×10 cm. No N_2O was observed but a large amount of $CO_2$ was found. The apparent quantum yield (no correction for the reaction $HO + NO \xrightarrow{M} HNO_2$) was 0.5. The indication is that either reaction (s) or reaction (t) occurs with a quantum yield of the order of magnitude of unity. Further work is being carried out.

Nitric acid.--The cross sections for absorption of ultraviolet radiation by nitric acid have been published by Johnston and Graham (1), and the values are entered in Table 1 and Figures 3 and 5. Quantum yields for the process

$$HNO_3 + h\nu \rightarrow HO + NO_2$$
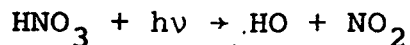
were determined by Johnston and Chang (18) in quartz cylinders with long exposure times to weak beams of monochromatic radiation and these results are reviewed here. Also, we photolyzed HNO_3

at 253.7 nm and observed the phase shift of NO_2 produced. The phase shift method (19) gave one molecule of NO_2 formed for one photon of 253.7 radiation absorbed by HNO_3, and the phase corresponded to a primary photochemical product. Thus at this one wave length we have a direct determination of unit quantum yield for NO_2 production from photolysis of HNO_3.

In a small quartz cylinder with long-term exposure of pure HNO_3 to monochromatic radiation, the quantum yield of NO_2 production is very low, about 0.1. The reason for this low quantum yield is that the products of nitric acid photolysis reform nitric acid under these conditions; the sequence of reactions is

$$HNO_3 + h\nu \rightarrow HO + NO_2$$

$$HO + HNO_3 \rightarrow H_2O + NO_3$$

$$NO_2 + NO_3 \overset{M}{\rightarrow} N_2O_5$$

$$\underline{H_2O + N_2O_5 \overset{W}{\rightarrow} 2HNO_3}$$

net: no change
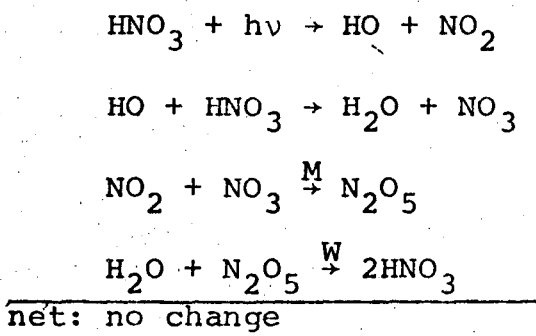
where M refers to energy-transfer catalysts in the gas phase and W refers to the walls of the apparatus. The small degree of reaction that is observed is caused by thermal and photochemical reactions involving N_2O_5 before it has a chance to react with water to reform HNO_3. Thus, long-term photolysis of pure nitric acid (20) vapor is an unsatisfactory method for studying the primary quantum yield for HNO_3 photolysis.

Upon addition of excess carbon monoxide to the nitric acid, the hydroxyl radical reacts with CO to produce CO_2

$$HNO_3 + h\nu \rightarrow HO + NO_2$$

$$HO + CO \rightarrow CO_2 + H$$

$$H + NO_2 \rightarrow NO + HO$$

$$\underline{HO + CO \rightarrow CO_2 + H}$$

$$\text{net:} \quad HNO_3 + h\nu \rightarrow NO + 2CO_2 + H$$
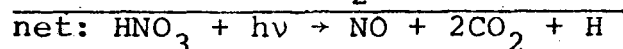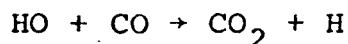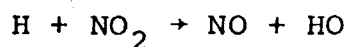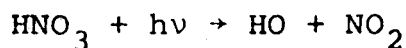
The interpretation of data in this system is somewhat ambiguous, since the fate of the final hydrogen atom is not known. If the second hydrogen atom does not react with nitric acid, the quantum yield to form carbon dioxide is two, and the primary quantum yield for nitric acid destruction can be inferred. On the other hand, if the hydrogen atom attacks nitric acid, for example,

$$H + HNO_3 \rightarrow HO + HNO_2$$

$$\underline{HO + CO \rightarrow CO_2 + H}$$

$$\text{net:} \quad HNO_3 + CO \rightarrow HNO_2 + CO_2$$
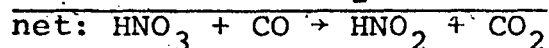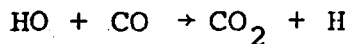
then the secondary processes represent a chain reaction with an indeterminate relation between observed CO_2 and primary quantum yield.

Upon addition of excess carbon monoxide and excess oxygen, the hydrogen atom is converted to the HOO radical, any nitric oxide formed is converted to nitrogen dioxide, and the significant secondary processes are

$$HNO_3 + h\nu \rightarrow HO + NO_2$$

$$HO + CO \rightarrow CO_2 + H$$

$$H + O_2 + M \rightarrow HOO + M$$

$$NO_2 + HOO \rightarrow HNO_2 + O_2 \quad \text{(reference 21)}$$

$$HNO_2 \xrightarrow[\text{time}]{HOO, \ O_2} NO_2 + \tfrac{1}{2}H_2O$$

$$\text{net: } HNO_3 + h\nu + CO + \tfrac{1}{4}O_2 \rightarrow CO_2 + NO_2 + \tfrac{1}{2}H_2O$$
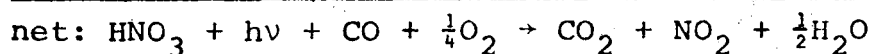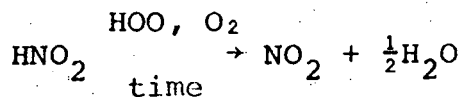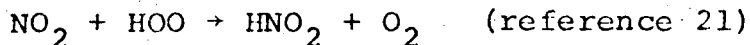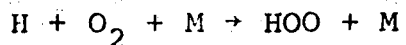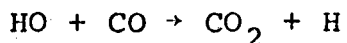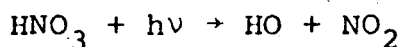
For large degrees of reaction, secondary photolysis of NO_2 forms NO, which reacts heterogeneously with nitric acid

$$NO + 2HNO_3 \xrightarrow{W} H_2O + 3NO_2$$
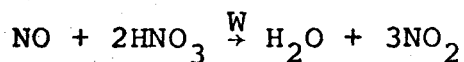
Another role of added excess oxygen is to suppress this reaction. Extensive model calculations (18) with up to 40 elementary reactions confirmed that no known secondary reaction destroyed HNO_3 or NO_2. With added CO and O_2, the quantum yield of CO_2 and NO_2 were each 1.0 at 200 nm, and that for NO_2 was 1.0 at 255 and 300 nm.

Acknowledgement

Table 1. Absorption cross sections, σ cm^2, for N_2O, NO_2, HNO_3, N_2O_4, and N_2O_5 at 5 nanometer intervals from 190 to 420 nm.

λ nm	N_2O	NO_2 10^{19} σ	HNO_3	N_2O_4 10^{19} σ	N_2O_5
190	1.26(-19)	6.12	1.32(-17)		
195		3.64	9.10(-18)		
200	4.46(-20)	3.19	5.50(-18)		
205		4.27	2.55(-18)		6.5(-18)
210	5.37(-21)	4.52	9.70(-19)		4.4(-18)
215		4.65	3.28(-19)		2.8(-18)
220	7.08(-22)	4.38	1.44(-19)		1.7(-18)
225		3.71	8.51(-20)		1.2(-18)
230	8.90(-23)	2.52	5.63(-20)		8.4(-19)
235		1.36	3.74(-20)		
240	1.90(-23)	0.90	2.60(-20)	10.7	5.2(-19)
245		0.39	2.10(-20)		
250	6.6(-24)	0.34	1.95(-20)	8.54	3.4(-19)
255		0.16	1.94(-20)		
260	4.67(-24)	0.18	1.90(-20)	7.97	2.1(-19)
265		0.24	1.80(-20)		
270	5.12(-24)	0.33	1.63(-20)	7.11	1.2(-19)
275		0.42	1.40(-20)		
280	6.02(-24)	0.57	1.14(-20)	5.69	6.3(-20) (a)
285		0.72	8.77(-21)		4.8(-20) (b)
290	5.0(-24)	0.88	6.34(-21)	4.12	4.2(-20)
295		1.07	4.26(-21)		
300	5.0(-24)	1.33	2.76(-21)	3.02	2.45(-20)
305		1.65	1.68(-21)	2.85	
310	3.2(-24)	1.97	9.50(-22)	3.02	1.3(-20)
315	1(-24)	2.24	4.70(-22)		
320		2.61	1.80(-22)	4.27	7.5(-21)
325		2.94	2(-23)		
330		3.38		6.12	4.0(-21)
335		3.61			

Table 1   (Con't.)

λ nm	N_2O	NO_2 10^{19} σ	HNO_3	N_2O_4 10^{19} σ	N_2O_5
340		4.17		6.90	2.7(−21)
345		4.30			
350		4.48		5.69	1.8(−21)
355		5.53			
360		4.96		3.20	1.0(−21)
365		5.84			
370		5.70		1.42	4.7(−22)
375		5.74			
380		6.52		0.57	1.3(−22)
385		6.45			
390		6.51		0.14	
395		6.08			
400		6.68			
405		6.52			
410		6.59			
415		6.03			
420		6.24			
425					
430					

(a)   This work, 205-280 nm.

(b)   Reference (10), 285-380 nm.

Table 2. Absorption cross section, σ cm^2, for the NO$_3$ radical at one nanometer intervals from 450 to 680 nm.

λ	$10^{19} \sigma$	λ	$10^{19} \sigma$	λ	$10^{19} \sigma$	λ	$10^{19} \sigma$
450		480	2.26	510	3.12	540	4.60
451	.51	481	2.24	511	3.80	541	4.44
452	.72	482	2.34	512	4.26	542	4.34
453	.57	483	2.24	513	4.08	543	3.54
454	.73	484	2.37	514	4.02	544	2.98
455	.61	485	2.33	515	3.79	545	3.70
456	.40	486	2.68	516	3.73	546	4.57
457	.51	487	2.73	517	3.57	547	6.13
458	.51	488	2.64	518	3.36	548	7.12
459	.56	489	2.73	519	3.35	549	6.53
460	1.03	490	2.87	520	3.77	550	6.13
461	1.07	491	2.87	521	4.21	551	6.13
462	1.19	492	2.76	522	4.53	552	6.06
463	0.92	493	2.84	523	4.62	553	6.21
464	0.67	494	2.61	524	4.06	554	6.47
465	0.95	495	2.65	525	3.72	555	7.02
466	1.06	496	2.89	526	3.64	556	7.52
467	1.16	497	3.20	527	3.79	557	7.74
468	1.32	498	3.22	528	4.62	558	7.99
469	1.34	499	3.16	529	5.51	559	8.41
470	1.60	500	2.97	530	5.80	560	8.43
471	1.99	501	2.81	531	5.39	561	7.65
472	2.13	502	2.71	532	5.01	562	7.17
473	2.00	503	2.63	533	4.67	563	6.94
474	1.82	504	2.97	534	4.61	564	6.74
475	2.01	505	3.19	535	5.14	565	6.69
476	2.27	506	3.29	536	6.18	566	6.77
477	2.48	507	3.25	537	6.53	567	6.84
478	2.60	508	3.04	538	6.08	568	6.90
479	2.38	509	2.81	539	5.13	569	6.88

Table 2 (Con't.)

λ	$10^{19}\ \sigma$	λ	$10^{19}\ \sigma$	λ	$10^{19}\ \sigma$	λ	$10^{19}\ \sigma$
570	6.79	600	6.83	630	14.9	660	12.0
571	6.73	601	6.45	631	12.6	661	23.3
572	6.69	602	6.71	632	8.73	662	34.7
573	6.65	603	7.76	633	6.00	663	40.2
574	6.67	604	8.92	634	4.59	664	29.1
575	6.95	605	9.78	635	3.57	665	18.5
576	7.42	606	9.05	636	3.29	666	13.4
577	7.80	607	6.90	637	3.87	667	8.59
578	7.81	608	4.98	638	4.26	668	5.46
579	7.67	609	4.09	639	4.03	669	3.96
580	7.67	610	3.82	640	3.10	670	3.34
581	8.01	611	4.06	641	2.86	671	2.58
582	8.10	612	4.47	642	2.79	672	2.50
583	7.42	613	5.33	643	2.28	673	2.25
584	6.79	614	5.67	644	2.31	674	2.14
585	6.61	615	5.46	645	2.20	675	2.17
586	6.96	616	4.87	646	2.20	676	2.07
587	8.30	617	4.44	647	2.31	677	2.21
588	10.3	618	4.47	648	2.22	678	2.71
589	12.4	619	4.89	649	2.20	679	2.55
590	13.4	620	5.67	650	2.17	680	2.63
591	12.8	621	8.35	651	2.11		
592	11.9	622	12.9	652	2.08		
593	10.8	623	22.0	653	2.31		
594	10.0	624	26.3	654	2.35		
595	9.44	625	21.1	655	2.59		
596	9.81	626	17.2	656	3.31		
597	10.0	627	15.4	657	4.10		
598	9.42	628	15.5	658	4.72		
599	7.94	629	15.3	659	6.73		

Table 3. Absorption cross section, σ cm^2, for nitrous acid vapor, HNO_2, at one nanometer intervals from 300 to 400 nm.

λ	$10^{20}\,\sigma$	λ	$10^{20}\,\sigma$	λ	$10^{20}\,\sigma$	λ	$10^{20}\,\sigma$
300	0.26	325	1.44	350	3.07	375	1.67
301	0.34	326	0.88	351	5.22	376	1.40
302	0.21	327	1.41	352	5.50	377	1.58
303	0.25	328	2.95	353	5.65	378	1.86
304	0.29	329	2.36	354	11.1	379	2.09
305	0.46	330	2.59	355	14.0	380	2.69
306	0.57	331	4.73	356	6.97	381	3.48
307	0.40	332	3.62	357	4.06	382	4.64
308	0.40	333	2.31	358	4.08	383	6.17
309	0.62	334	2.65	359	3.72	384	7.38
310	0.58	335	2.93	360	3.11	385	6.96
311	0.60	336	2.40	361	2.52	386	5.10
312	0.92	337	1.69	362	2.62	387	3.27
313	0.94	338	2.39	363	2.84	388	2.23
314	1.23	339	4.93	364	3.89	389	1.54
315	1.39	340	4.17	365	4.87	390	1.04
316	1.17	341	4.28	366	5.70	391	0.67
317	1.47	342	9.43	367	8.03	392	0.52
318	2.14	343	7.34	368	13.4	393	0.47
319	1.93	344	3.66	369	14.4	394	0.31
320	1.55	345	3.21	370	8.67	395	(0.14)
321	1.94	346	3.40	371	4.69	396	(0.13)
322	1.42	347	3.28	372	3.39	397	(0.12)
323	1.09	348	2.77	373	2.88	398	
324	1.54	349	2.61	374	2.10	399	

References

1. H.S. Johnston and R. Graham, J. Phys. Chem. 77, 62 (1973).

2. C.E. Dinerman and G.E. Ewing, J. Chem. Phys. 53, 626 (1970).

3. D.R. Bates and P.B. Hayes, Planet. Space Sci. 15, 189 (1967).

4. K.F. Preston and R.F. Barr, J. Chem. Phys. 54, 3347 (1971).

5. R.F. Hampson, Ed., Chemical Kinetics Data Survey VI. NBSIR 73-207, pp. 59-78 (May 1973).

6. T.C. Hall, Jr. and F.E. Blacet, J. Chem. Phys. 20, 1745 (1952).

7. H.H. Holmes and F. Daniels, J. Am. Chem. Soc. 56, 630 (1934).

8. F. Daniels and E.H. Johnston, J. Am. Chem. Soc. 43, 53 (1921).

9. H.J. Schumacher and G. Sprenger, Z. Physik. Chem. B2, 267 (1929).

10. E.J. Jones and O.R. Wulf, J. Chem. Phys. 5, 873 (1937).

11. R.F. Murphy, "The Ultraviolet Photolysis of the Nitrogen Oxides", Ph.D. Dissertation, University of California in Los Angeles (1969).

12. R.F. Hampson, Ed., Chemical Kinetics Data Survey VI. NBSIR 73-207, pp. 93-97 (May 1973).

13. H.S. Johnston, "Gas Phase Reaction Rate Theory". The Ronald Press Company, New York (1966).

14. G. Schott and N. Davidson, J. Am. Chem. Soc. 80, 1841 (1958).

15. D.A. Ramsay, "Optical Spectra of Gaseous Free Radicals", Spectroscopy, pp. 593-595.

16. a. A.P. Altshuller, J. Phys. Chem. 61, 251 (1957); b. D.M. Waldorf and E.L. Balb, J. Chem. Phys. 39, 432 (1963).

17. G.W. King and D. Moule, Canad. J. Chem. $\underline{40}$, 2057 (1962).

18. H.S. Johnston and S.G. Chang, submitted to J. Phys. Chem. 1973.

19. H.S. Johnston, G.E. McGraw, T.T. Paukert, L.W. Richards, and J. van den Bogaerde, Proc. Nat. Acad. Sci. $\underline{57}$, 1146 (1967).

20. T. Berces and S. Forgeteg, Trans. Faraday Soc. $\underline{66}$, 633 (1970).

21. R. Simonaitis and J. Heicklen, private communication.

Figure Captions

Figs. 1-5. Absorption cross sections, σcm^2, as a function of

wavelength with principal, energetically possible primary

dissociation fragments.

Fig. 1. Nitrous oxide, N_2O.

Fig. 2. Nitrogen dioxide, NO_2, and portions of the N_2O spectrum.

Fig. 3. Dinitrogen pentoxide, N_2O_5, ----, Jones and Wulf;

———, this study. Nitric acid, HNO_3.

Fig. 4. NO_3 radical and the visible spectrum of ozone, O_3, for

comparison (NO_3 is prepared from N_2O_5 plus excess O_3).

Fig. 5. Nitric acid, HNO_3, and nitrous acid, HNO_2.
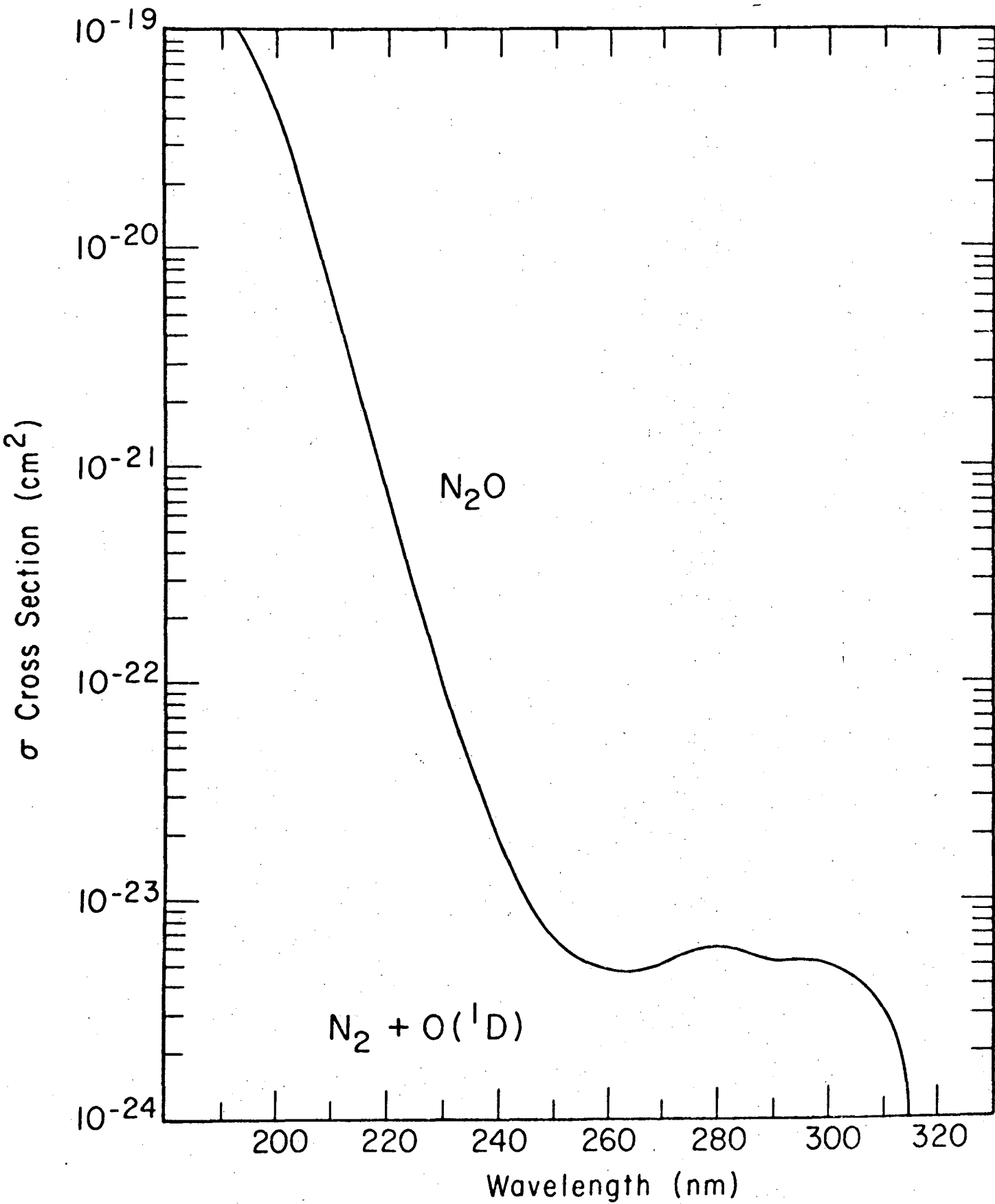
Fig. 1

XBL 738-1684

Fig. 2

Fig. 3

XBL 738-1682

Fig. 4

XBL 738-1683

Fig. 5